Journal of the Korean Physical Society, Vol. 63, No. 4, August 2013, pp. 867∼876 Review Articles

Review of Cold Rydberg Atoms and Their Applications

Jongseok Lim, Han-gyeol Lee and Jaewook Ahn*
Department of Physics, Korea Advanced Institute of Science and Technology, Daejeon 305-701, Korea

(Received 25 February 2013, in final form 27 March 2013)

We present an introductory review of the latest advancements cold Rydberg atom research. First, we briefly summarize the exaggerated properties of Rydberg atoms, and we discuss the new perspectives of Rydberg atom research that has been enabled by laser cooling and trapping technique. We then highlight the latest developments and achievements in the newly emerged research fields for Rydberg molecules and cold neutral plasmas. Various applications of the Rydberg blockade effect for quantum optics and quantum information science are also reviewed.

PACS numbers: 36.90+f, 39.25+k, 32.10-f
Keywords: Ryderg atoms, Atom cooling and trapping, Rydberg blockade effect
DOI: 10.3938/jkps.63.867

I. INTRODUCTION

Rydberg atoms are atoms in their highly excited energy states [1–3]. The study of Rydberg atoms has a long history in physics, dating back to more than a century ago when the high-lying energy levels of hydrogen in the Balmer series were first studied in atomic spectroscopy to become the experimental ground for the Bohr's atom modeling [4, 5]. Helped by the gradual development of sophisticated experimental techniques in high-resolution absorption spectroscopy, the bizarre nature of Rydberg atoms has become uncovered piece by piece and has drawn keen interest ever since. The physical properties of Rydberg atoms are particularly important in the presence of external fields [6,7] or during the collision or ionization process, and their extreme properties have been under intense investigation [8–10].

Research involved with Rydberg atoms has real applications: One of the examples is found in astrophysics [11,12], where radio and microwave frequency transitions of Rydberg states correspond to radiative recombination of low-energy electrons and ions in interstellar media. Another application based on the dynamics of Rydberg atoms, which can be extremely slow with respect to the time resolution of ultrafast laser spectroscopy and has been used to unveil the link between the stationary description of quantum wave functions and the classical orbiting dynamics of electron wave-packets around atomic ions [13–15]. Furthermore, the lately applauded by the Nobel physics prize in 2012, the long-lifetime and huge electric dipole moment of Rydberg atoms in a high-Q resonant cavity led to the counting emitted microwave photons, allowing the quantum non-demolition photon state measurements [16,17].

In the context of the subject for which this review article was prepared, cold Rydberg atom research is based on the technique of laser cooling and trapping of atoms. With the advent of technology of laser cooling and trapping of atoms [18,19], a new perspective for Rydberg atom research has become enabled. Within a cold atomic vapor, the kinetic motions of atomic nuclei are almost frozen during the long radiative lifetime of Rydberg states, and hence the fascinating features of strong interactions between Rydberg atoms can be directly observed experimentally. First, many-body effects on resonant dipole-dipole energy transfer resulted in diffused excitation line profiles in the temperature region where atoms are cooled to an energy neraly to their thermal energy [20, 21]. Cold Rydberg atom clouds have also been found spontaneously to transform into an ultracold plasma state, where strikingly the translationally-bound cloud of cold ions trapped electrons to further ionize other Rydberg atoms to make the as-formed plasma further expand [22]. More recently, the strong coupling between a pair of Rydberg atoms or between a Rydberg atom and a ground state atom manifests itself in the formation of an exotic molecular state with a mesoscopic intermolecular distance [23–27].

The Rydberg atom dipole blockade or the inhibition of multiple Rydberg excitation is of particular importance in quantum optics and quantum information [28]. In recent experiments, strong interaction has been observed to appear between a pair of trapped atoms when they are excited to a Rydberg state within the dense atomic vapor region. This paired-atom interaction in the dipole blockade is often used to implement two-qubit entangled quantum gates [29]. A large experimental effort is nowadays being devoted to further extend the applicability of

*E-mail: jwahn@kaist.ac.kr; Fax: +82-42-350-2510

Rydberg dipole blockade in various research fields including non-classical state engineering, quantum nonlinear optics, quantum error correction, quantum communication, and quantum computing [30]. For the implementation of scalable quantum information processor, various experimental platforms for Rydberg atom spatial configuration are under consideration, which include, for example, spatially-ordered Rydberg atoms in large-spacing optical lattices, or magnetic trap arrays [31–33].

Another entrancing observation may be the discovery of collective quantum states in an ensemble of cold atoms excited into Rydberg states [34]. The strongly-correlated many-body states, in which Rydberg excitations were coherently distributed among all atoms, formed a crystalline spatial distribution of collective excitation. The laser-excited two-dimensional Rydberg atomic Mott insulator phase was directly imaged by using a high-resolution *in situ* Rydberg atom imaging system.

In this review article, we provide an introductory overview of the most important topics in this fast evolving young research field of cold Rydberg atoms. We intend to summarize each topic with a brief description of the fundamental principle and with the most up-to-date experimental demonstrations. However, we need to mention that a number of seminal review articles on various specific topics such as Rydberg atoms in external fields [7], Rydberg atom interactions [35, 36], quantum information application of Rydberg atoms [30], and ultra-cold plasmas [37] already exist. Still, the reason we prepared another review article on cold Rydberg atoms was in part because the development speed of this fast-growing research field allowed another up-to-date worthwhile review article and in part because this invited article was prepared as part of the special topical edition of articles on cold atoms and molecule research in the Journal of the Korean Physical Society.

The paper is structured such that Sect. II provides the basic scaling properties of Rydberg atoms as a function of the principal quantum number n, and Sect. III briefly describes the experimental procedure of producing Rydberg atoms. In Sects. IV and V, we discuss the principles and the experimental achievements related with Rydberg molecules and ultra-cold neutral plasmas, respectively. After describing the principles of the Rydberg atomic dipole blockade in Sect. VI, we discuss the basic ideas and prospects of various Rydberg atom-based quantum information processing proposals and realizations in Sect. VII. We conclude by discussing some possible future directions of this fast-growing young research field.

II. PROPERTIES OF RYDBERG ATOMS

The physical properties of Rydberg atoms are well described in monographs, for example, in Ref. 1. Briefly to summarize, Rydberg atoms exhibit incredibly exaggerated features compared to those of conventional atoms in their ground state or in their first few excited energy states. Due to the huge size of these atoms, which scales as n^2, where n is the principal quantum number, the dipole moment, for example, scales as $\mu_n \propto n^2$, and the radiative lifetime scales as $n^3(l+1/2)^2$, where l is the angular quantum number. The physical properties, which are proportional to the area of the atomic orbit, such as the geometric cross section and diamagnetic energy shifts, therefore scale as n^4. For a Rydberg atom with $n = 50$, therefore, the atom size approaches the typical size of a bacteria of 1 μm, and the radiative lifetime extends to near 100 μs. A few frequently used physical properties of the rubidium atom in the $50p$ state are estimated in Table 1 to summarize the scaling properties of Rydberg atoms. Recent measurements of the Rydberg state lifetimes carried out in cold rubidium Rydberg atom in a magneto optical trap (MOT) reported 64 μs for $60p_{3/2}$, which extended the earlier thermal sample measurements, that had been limited below $n \approx 20$ by avoiding the finite-detection-volume and collision-depopulation effects [38–40].

Rydberg energy states of alkali-metal atoms are well described by the Bohr atom picture of a valence electron orbiting around a positively-charged atomic core. As the atomic core is screened by core electrons, an empirical formula for the binding energy is given by

$$E_{n,l,j} = E_\infty - \frac{Ry}{(n-\delta_{n,l,j})^2}, \tag{1}$$

where Ry is the Rydberg constant, E_∞ is the ionization energy limit, $\delta_{n,l,j}$ is the so-called quantum defect [41,42], which describe the discrepancy of a Rydberg atomic state from that of a hydrogen atom, and j is the total angular quantum number. Thus, the binding energy scales as n^{-2}, to be more precise as $(n^*)^{-2}$, where $n^* = n - \delta_{n,l,j}$. Then, the energy difference between adjacent n states scales as $\Delta_n \propto n^{-3}$, so, the polarizability given by $\alpha_0 \propto \mu^2/\Delta$ scales as n^7. Traditionally, accurate measurements of the polarizability of Rydberg atoms are hindered by thermal collisions, but recent measurements carried out in a cesium MOT have produced a scaling law of the polarizability of Rydberg atoms up to $n = 50$, where the strong long-range interaction between Rydberg atoms of scaling in n^{11} started to play a role [43–45].

In the presence of external fields, the properties of Rydberg atoms show striking sensitive responses [7]. As the binding energy of a Rydberg atom is small, even a moderately-low electric field causes valence electrons to escape easily over the Coulomb potential barrier [46]. The classical ionization field, denoted by F, is obtained at the saddle point condition of the Stark-Coulomb potential given by

$$F = \frac{1}{16n^4} \tag{2}$$

in atomic units, which is about 50 V/cm for $n = 50$, without considering linear Stark energy level shift [1].

Table 1. Scaling properties of Rydberg atoms [1].

Property	n-scaling	Rb ($50p$)
Binding energy	n^{-2}	6.2 meV
Energy between adjacent n states	n^{-3}	0.22 meV
Radiative lifetime	n^3	106 μs
Fine-structure interval	n^{-3}	-0.9 MHz
Orbital radius	n^2	0.17 μm
Dipole moment $\langle np\|er\|nd\rangle$	n^2	3200 ea_0
Geometric cross-section	n^4	0.096 μm^2
Scalar polarizability	n^7	$\sim$GHz cm^2/V^2

On the other hand, when the Stark shift is included, the result in Eq. (2) is changed to $F = 1/9n^4$. When the Stark energy levels shift so severely that different n energy levels experience avoided-crossings, which occurs for an ac electric field of $F > 1/3n^5$, a different kind of ionization occurs, for example, multi-photon ionization by microwave fields [47]. The effects of magnetic fields on Rydberg atoms are highlighted by the presence of quasi-Landau resonances above the ionization limit which shows a series of sharp resonances at frequency intervals of $3\omega_c/2$, where $\omega_c = eB/mc$ is the electron cyclotron frequency [48]. Recently, magnetic trapping of cold Rydberg atoms has revealed collective oscillations of cold atoms, showing extremely long Rydberg gas lifetimes of up to 200 ms [49,50].

III. EXPERIMENTAL REALIZATIONS

The production of cold Rydberg atoms typically starts with laser cooling and trapping of neutral atoms. There are many good reference books and articles for the method of laser cooling and trapping of atoms [18, 19]. In a MOT with a configuration of three pairs of counter-propagating laser beams and magnetic fields, as many as 10^9 atoms can be cooled to a temperature below mK and can be spatially confined at a atom density of 10^{10-11} cm^{-3}.

For a rubidium system, a trapping laser, typically a narrowband diode laser at 780 nm, red-detuned by about the natural linewidth from the cooling transition $5s_{1/2}$(F=2) $\rightarrow$ $5p_{3/2}$(F'=3), while being frequency-stabilized with respect to the saturation absorption spectrum of a reference rubidium, is used. Also, a re-pump laser, a narrowband diode laser, drives a re-pumping transition, $5s_{1/2}$(F=1) $\rightarrow$ $5p_{3/2}$(F'=2), to achieve a two-level system consisting of $5s_{1/2}$(F=2) and $5p_{3/2}$(F'=3) hyperfine energy levels. Then, with the trapped atomic cloud in a volume of 1 mm^3 in the MOT, Rydberg atoms are created. First, the trapping laser is tuned to the resonant frequency of the two-level system, and the atoms prepared in $5p_{3/2}$(F'=3) are then excited to one of the Rydberg energy levels of rubidium by using a Rydberg

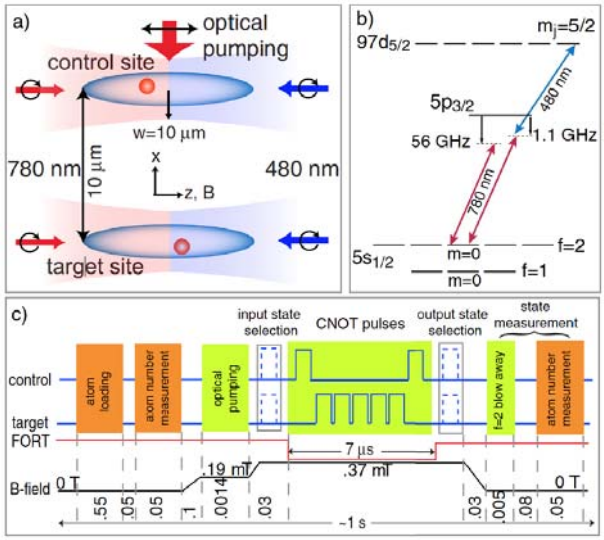

Fig. 1. (Color online) Experimental scheme for the observation of the Rydberg blockade effect in a pair of FORTs: (a) Illustrative experimental configuration, (b) energy levels and laser excitation frequencies, and (c) the laser operation time sequence to perform a C-NOT gate operation as explained in Sec. VII. . The image is from Ref. 52 with permission of the publisher.

excitation laser. After the Rydberg excitation laser is switched on for a time period of about 20 μs within the Rydberg atom's lifetime to accumulate Rydberg atoms, the Rydberg excitation laser is then switched off and the trapping laser is reset to the trapping laser's frequency. The detection of the Rydberg atoms is carried out by field ionization by applying the ionization electric field of the Rydberg atoms to the parallel plates across the atom cloud [20,21].

Most of the reported Rydberg atom-related experiments have been carried out in MOT systems described in the previous paragraph. However, in more recent experiments, in particular, those designed for the study of Rydberg atom interactions, single-atom monitoring capability has become essential, so different types of experimental environments for Rydberg atom research are considered. As an example, Fig. 1 shows the experimental geometry of the Rydberg atom pair interaction experiments in far-off-resonance optical traps (FORTs) [51]. In the FORTs setup, the dipole blockade effect between two Rydberg atoms is studied, where two infrared beams of moderate laser power are focused to spatially adjacent sites of 10 μm apart from each other so that a few mK-deep potential wells are formed at the foci with a focused radius of a few μm in each individual beam. After being initially loaded and cooled in the MOT, the atoms are captured in FORT sites, and the trap and repump beams are turned off to remove the atoms untrapped in the FORTs. Then, within the lifetime of FORT loading, various experiments can be performed, *e.g.,* experiments on the Rydberg dipole blockade interaction [29]

and Rydberg quantum gate implementation [52], where the light scattered off the trapped atoms is collected through a high-numerical-aperture lens onto the screen of a sensitive charge-coupled-device (CCD) camera for site-specific image detection of single atoms.

IV. RYDBERG MOLECULES

Rydberg atoms have enormous polarizability that scales as n^7, which results in discovery of new kinds of exotic molecules. These Rydberg molecules are different from the conventional Rydberg molecules or the molecules in high-energy Rydberg states which are often studied in zero-kinetic energy photoelectron spectroscopy. These new kinds of Rydberg molecules can be created in laser cooled atomic vapors by photo-assisted chemical bonding between Rydberg atoms and ground-state atoms [24].

Rydberg atoms can have large permanent and induced dipole moments, so they are strongly influenced by van der Waals and dipole interactions, respectively. The interaction between Rydberg atoms is largely determined by Coulomb interactions, along with higher-order corrections, aside from the chemical exchange overlap interaction acting only over extremely-short distances of less than a few nm. Thus, the electric potential of molecular states as a function of the inter-atomic distance R can be given by

$$V(R) = D_e + \sum_n \frac{C_n}{R^n}, \tag{3}$$

where D_e is the dissociation energy and C_n are the coupling constants. When permanent electric dipole moments are present, the dominant dipole-dipole coupling contribution turns out to be the C_3/R^3 term and the C_3 coefficient is proportional to the square of the dipole matrix element. However, when the permanent dipole moments are not present, for example, in the homonuclear molecular ground states, the leading contribution in an asymptotically approaching ns+ns bi-atomic ground state at long range becomes C_6/R^6. Hence, the van der Waals energy or the interaction between induced dipoles dominates at long range. In this case, the dispersion coefficient is given by $C_6 = -(\mu_1\mu_2)^2/\Delta$, which scales as n^{11}, where Δ is the aforementioned energy difference between adjacent energy levels.

The strong interaction between Rydberg atoms was observed first in Rydberg dipole blockage experiments [52, 53] and later more clearly in long-range Rydberg molecular resonance experiments. In the latter, molecular resonance features were found in the excitation spectra of ultra-cold atoms of rubidium and cesium in their Rydberg states [54, 55]. Also, when an atom in a Rydberg state interacts with a nearby ground state atom or molecule, Rydberg macro-molecules can be formed, being bound together at large distances of thousands of Bohr radii. In this case, the governing interaction can be derived from simple electron scattering off the ground-state species, and, because the electron kinetic energy is so low, the electron scattering is primarily s-wave. Therefore, the main physics can be manifested by the s-wave scattering length. Recent studies have shown that a low-energy Rydberg electron interacting via the zero-range Fermi pseudo-potential with a nearby atom could have a negative scattering length and bind into ultra-long-range Rydberg molecular states [23].

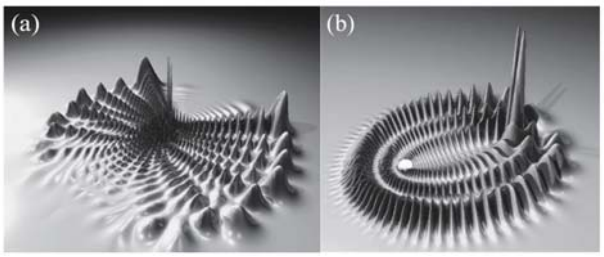

Fig. 2. Electronic probability densities of a "butterfly molecule" and a "trilobitemolecule" on a constant θ surface in cylindrical coordinate system. (a) The p-wave scattered-state Rydberg molecule consists of an $n = 30$ Rb atom, and a nearly ground-state Rb atom is distributed with the shape of butterfly wings. The highest peaks are located at the position of the nearly ground-state Rb atom. (b) Rb($30d$) + Rb($5s$) Rydberg molecule, in an s-wave scattered state, exhibits the triolobite shape. The position of the Rb($5s$) atom is located under the "twin tower", and the position of the Rb^+ ion is illustrated as a small white sphere. The asymmetrical electronic probability density gives a permanent dipole moment of about 0.3 kdebye. The images are from Refs. 25 and 26 with permission of the publishers.

Furthermore, for Rydberg atoms with low orbital angular momenta, Rydberg molecules were predicted to form in their triplet states $^3\Sigma(5s - ns)$ of Rb_2, where $n = 35 - 37$, and these Rydberg molecules have been experimentally observed with 20-μs molecular lifetimes [24]. These Rydberg molecules are often called "butterfly molecules" due to their shape (see Fig. 2(a) [25]). On the other hand, for Rydberg atoms with high-angular-momentum quasi-degenerate energy states, the Rydberg electron interaction with the core electrons works as an energy shift of the Rydberg states from their unperturbed hydrogenic energy levels, and the deep hydrogenic potentials can result in more bound vibrational states. Under this given senarario, a second class of Rydberg molecules, often referred to as "trilobite molecules" (see Fig. 2(b)), is predicted. These molecules possess permanent electric dipole moments given by $\mu = R - n^2/2$ (atomic unit), albeit the fact that they are homonuclear diatomic molecules [26].

Another kind of, and even more exotic, Rydberg molecule exists when the ground-state atom in the previous Rydberg molecules is replaced by a polar molecule. This type of molecules is predicted to be formed when

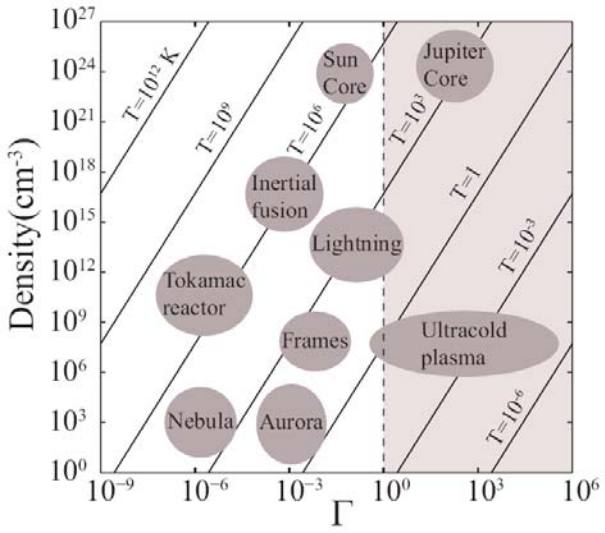

Fig. 3. (Color online) Neutral plasmas in nature compared with an ultra-cold neutral plasma. The ultra-cold neutral plasma enables strongly-coupled ($\Gamma > 1$) ion research in previously unchartered temperature and density ranges [37].

Rydberg atoms interact with polar molecules. These are macro-polyatomic molecules formed under an ultra-cold temperature environment and possible candidates for the polamolecules are KRb's and deuterated hydroxyl (OD)'s. As these giant molecules are involved with an anisotropic charge-dipole interaction that scales as extremely long-ranged $1/R^2$, they are polarized being as a dipole in a double-well energy potential [27].

V. ULTRA-COLD NEUTRAL PLASMAS

Ultra-cold neutral plasmas are created in the environment of a cold atomic vapor in conjunction with laser ionization [56]. Particular interest has been drawn from the scientific community because ultra-cold neutral plasmas are characterized by their occupying an exotic research regime of plasma physics [22, 56]. As illustrated in Fig. 3, the ultra-cold neutral plasmas differ from other plasma sources: They are extremely dilute, $\rho = 10^{6-10}$ cm^3, but they still satisfy the strong coupling condition because they have a cold temperature below mK [37]. In the strong-coupling region, or

$$\Gamma = \frac{e^2}{ak_BT} > 1, \tag{4}$$

where a is the Wigner-Seitz radius characterizing the particle separation in a plasma [57], the Coulomb interaction energy between particles exceeds the average kinetic energy. Under these interaction and kinetic energy conditions, collective dynamics can emerge as a result of the presence of a spatial correlation of the plasma [58]. In particular, the low density of the ultra-cold plasma facilitates an extremely slow characteristic time scale, so transient plasma phenomena have been observed. They include plasma formation and expansion [59], recombination to Rydberg atoms [22], collective plasma-wave propagations, and plasma instabilities [60].

Ultra-cold neutral plasmas are created either by using a photo-ionization process of cold atoms or by using a photo-excitation process of the cold Rydberg state atoms. Electrons liberated by subsequent inelastic collisions or blackbody radiation are trapped by the resulting positive background charges to form a plasma in an admixture of electrons in temperatures from 1 to 1000 K and ions at 1 K [37]. Ultra-cold neutral plasmas have been experimentally created by many research groups: The tested atomic species to be formed into ultra-cold neutral plasmas include xenon, strontium, calcium, rubidium, cesium, and even rubidium BEC [22,61–65].

The plasma formation and expansion dynamics are divided into three distinct phases: In the first phase, cold atoms are photoionized, and the photoliberated energetic electrons quickly escape from the atoms within 10 ns. Following the fast event, more electrons are ionized from Rydberg atoms via blackbody radiation and start to leave the atomic cloud slowly in a 1 μs time scale. However, in the second phase, the electrons are trapped in a huge attractive Coulomb potential formed by the background ions, and an avalanche process of ionization occurs until an equilibrium state of ions is formed. This process takes place on a time scale of 10 μs, which is equivalent to the inverse of the ion plasma frequency. Lastly, the as-formed plasma slowly expands until the so-called hydrodynamic time-scale elapses. The hydrodynamics time is given by

$$\tau = \sqrt{\frac{m\sigma^2}{k_BT_e}}, \tag{5}$$

where T_e is the electron temperature and σ is the size of the plasma, which is over 100 μm in a typical ultra-cold neutral plasma.

In the ultra-cold neutral plasma, one can observe various collective oscillations. The first one is the electron plasma oscillation, known as the Tonks-Langmuir mode, which represents an electron density oscillation in a quasi-neutral plasma or metals. Its frequency is described, when the thermal motion of the electrons is ignored, by ω_{TL} given by

$$\omega_{TL} = \sqrt{\frac{e^2n_e}{\epsilon_0 m_e}}, \tag{6}$$

where n_e is the electron density, ϵ_0 the vacuum permittivity, and m_e the electron mass. This mode can be resonantly excited by using a radio frequency electric field that pumps energy into the plasma and further increases the plasma temperature. The phenomenon has been observed in early experiments of electron plasma oscillation measurements. In that, the resonant frequency of

the electron plasma oscillation was shifted to lower frequency as the plasma expansion progressed [59]. When the thermal effect becomes important in an inhomogeneous electron distribution of plasmas, another electron density wave known as the Tonks-Dattner mode, whose frequency ω_{TD} is given by

$$\omega_{TD}^2 = \omega_{TL}^2(r) + \frac{3k_B T_e}{m_e} k^2(r), \tag{7}$$

where $k(r)$ is the local wavenumber, was predicted and also observed experimentally [66,67].

There also exist electrostatic waves of longitudinal ion density oscillations, which, long with Langmuir oscillations, are considered to be fundamental waves in plasma physics. In a hydrodynamic approximation in which ions are assumed to move slowly and the electron density is assumed to be isothermally uniform, it is predicted that the dispersion relation for the ion density oscillation is given by

$$\omega_{ion} = \sqrt{\frac{k_B T_e / m_{ion}}{k^{-2} + \lambda_D^2}}, \tag{8}$$

where λ_D is the Debye screening length, and k is the wave vector. Recent experiments adopting a technique of initial density shaping of a periodic modulation in an ultracold neutral plasma has reported ion acoustic wave excitations and even electron correlation effects on collective ion oscillations [68,69].

VI. RYDBERG ATOM DIPOLE BLOCKADE

When two atoms interact strongly with each other, their simultaneous excitation to the same Rydberg state by an instant driving field may be forbidden, because the presence of the first atom excitation to the Rydberg state detunes the Rydberg energy level of the second atom [44, 45]. This phenomenon is known as Rydberg atom dipole blockade of excitation, and was proposed in a decade ago for quantum information processing with neutral atoms [28,70]. As an elementary building block of quantum information processing circuits, the dependence of a conditional excitation of a qubit on the other qubit's energy state allows the two-bit logical operation known as C-NOT [71].

To explain the principle of Rydberg atom dipole blockade, as shown in Fig. 4, we consider two atoms separated by a distance R and both in the ground state, *i.e.,* $|g, g\rangle$. When one of the two atoms is excited to a Rydberg state, *i.e.,* $|r, g\rangle$, the excitation to the same Rydberg state, *i.e.,* $|r, r\rangle$, of the other atom located within a distance smaller than the so-called blockade radius R_b is blockaded [29, 53]. This is due to the Rydberg interaction energy between the two atoms, which shifts the doubly-excited state of the two atoms $|r, r\rangle$ off resonant. In other words,

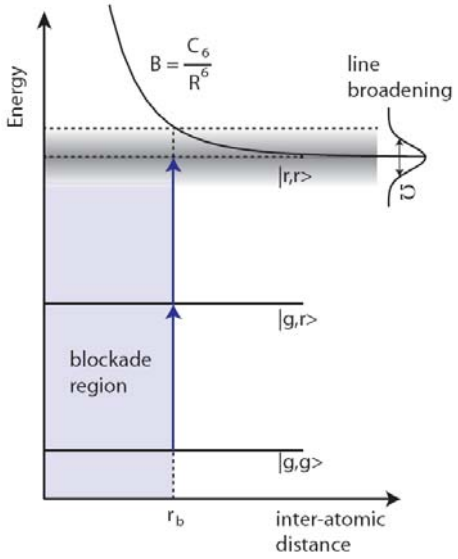

Fig. 4. (Color online) Schematic representation of Rydberg blockade excitation. When an electric field with a coupling strength Ω induces a transition between $|g\rangle$ and $|r\rangle$, the van der Walls interaction shifts the energy level, B, of the coupled state $|r, r\rangle$ as a function of inter-atomic distance R ($B = C_6/R^6$). When the blockade shift B is bigger than the linewidth of the transition, the transition from $|r, g\rangle$ to $|r, r\rangle$ is inhibited. Here, the linewidth is determined by the Rabi frequency Ω.

the blockade shift B is bigger than the linewidth of the coupling laser field, or in terms of Rabi frequency Ω,

$$B \gg \Omega. \tag{9}$$

where the power broadening of the two-level system is proportional to the Rabi frequency in the regime where the Rabi oscillation occurs on a time much shorter than the natural decay time [72]. As previously discussed, the Rydberg interaction scales as n^4/R^3 in the dipole-dipole interaction regime for $R < R_c$, where R_c is the crossover inter-atomic distance, and as n^{11}/R^6 in the van der Waals interaction regime for $R > R_c$. For Rydberg levels of $n = 60 \sim 80$, the van der Waals interaction is relevant because R_c varies within a few μm, which is sufficiently small compared to the experimental size of cold atom samples. Therefore, $B \simeq \frac{C_6}{R^6}$, and the blockade radius R_b for the two-atom van der Waals interaction is given by

$$R_b \sim \left(\frac{C_6}{\Omega}\right)^{1/6} \tag{10}$$

because the blockade shift B should suffice the condition $B > \Omega$.

In rubidium atoms, Rydberg levels of $n = 80$ provide a blockade shift of $B/2\pi > 3$ MHz at a blockade radius of $R_b = 10$ μm, which distance is well within the controllable range of individual atoms, for example, by means

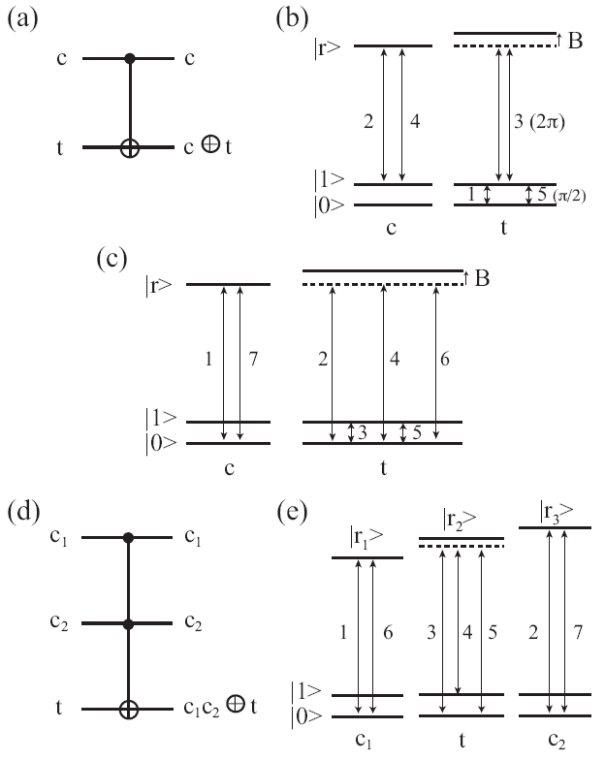

Fig. 5. (a) C-NOT gate, and (b) the five-pulse implementation and (c) the seven-pulse implementation of the C-NOT gate in a two-Rydberg-atom system. (d) Toffoli gate, and (e) the seven-pulse implementation of a Toffoli gate in a three-Rydberg-atom system.

of optical tweezing of an atom pair in a pair of tightly focused beams of a far-detuned laser. Experimental realizations of two-atom Rydberg blockade were performed both in the dipole-dipole interaction region for rubidium $n = 90$ at $R > 10$ μm [29] and in the van der Waals interaction region for $n = 58$ at $R \sim 3.6$ μm [53].

The dipole blockade at the Föster resonance has also been observed, and corresponds to the resonant dipole-dipole energy transfer of the np+$np \rightarrow ns$+$(n+1)s$ reaction [73]. In the experiment, the dipole-dipole interaction of atomic cesium in n=20 - 25 was tuned on and off by using the Stark effect, and the excitation of a pair of atoms at the Föster resonance occurred as a result of an avoided crossing between the energy levels of the pair of np+np atoms and ns+$(n+1)s$ atoms.

In a two-dimensional or three-dimensional optical dipole trap array, on the other hand, many adjacent atom sites can be located within the blockade radius, and a simultaneous laser illumination on an ensemble of N atoms allows only one Rydberg atom to be excited inhibiting at the same time the rest of the atoms from being excited. Provided all the atoms are strongly interacting with each other, which atom is excited is completely undecided; hence, the excited state of the ensemble must be described by a coherent superposition state, $|R\rangle$, of all possible N particle states of a single excited atom and $N-1$ atoms in the ground state in such a way that

$$|R\rangle = \frac{1}{\sqrt{N}} \sum_{i=1}^{N} |g_1, g_2, \cdots r_i, \cdots, g_N\rangle, \tag{11}$$

where i is the index of the atom excited to the Rydberg level. In the given system described by an N-particle collective wave function, the single-atom excitation is N times more probable than it is in an isolated single-atom system, so the Rabi oscillation frequency between the ground state $|g_1, g_2, \cdots, g_N\rangle$ and the excited collective N-particle state $|R\rangle$ is given by

$$\Omega = \sqrt{N}\Omega_1, \tag{12}$$

where Ω_1 is the corresponding single-atom Rabi oscillation frequency [28,74]. Therefore, the Rabi frequency for the N-particle coherent excitation in the Rydberg dipole blockage regime is $\sqrt{N}$ times bigger than the single-atom Rabi oscillation frequency.

For a cold atom cloud of uniform density ρ, the number of strongly-interacting atoms is given by $N \sim \rho R_b^3$, and from Eqs. (10) and (12), the blockade radius is given by $R_b \sim (C_6/\sqrt{N}\Omega_1)^{1/6}$ for the van der Waals interaction, so the number of interacting atom scales in terms of the density as $N \sim \rho^{5/4}$, and the Rabi frequency $\Omega_N \sim \rho^{5/8}$. Likewise, for the $1/R^3$ dipole-dipole interaction, the scaling of the N-[article Rabi oscillation frequency becomes $\Omega_N \sim \rho^{1/3}$ [75].

VII. RYDBERG ATOM QUANTUM COMPUTING

Quantum information processing requires quantum-mechanical ways of storing, processing, and retrieving information. When neutral atoms are considered to process quantum information, a quantum-mechanical bit, a so-called qubit, is often realized with two hyperfine ground-state energy levels labeled by $|0\rangle$ and $|1\rangle$ because they are stable and robust against environmental perturbations. Single qubit operations are relatively easy to implement by means of, for example, optical two-photon transitions that induce changes between any superposition states of $|0\rangle$ and $|1\rangle$ [76]. Nonetheless, together with the single-qubit operations, a two-qubit controlled NOT (C-NOT) gate operation is necessary to construct a minimal set of quantum operations sufficient to perform any arbitrary unitary operations; thereby, the C-NOT gate implementation is of great importance in realizing universal quantum computation [71].

The C-NOT gate has two input qubits, known as the "control" qubit and the "target" qubit, respectively. The logical circuit representing the C-NOT is shown in Fig. 5(a), where the top line represents the control qubit while the bottom represents the target qubit. The gate's

operation depends on the state of the control qubit, and if the control qubit is 0, the target qubit is unchanged, but if the control qubit is 1, the target qubit is flipped between 0 and 1.

Rydberg atoms have drawn significant interest in quantum-information community as a good candidate for neutral-atom-based quantum information processing [28, 70]. The reason is simply that because of the Rydberg dipole blockade effects, two-qubit operations, such as the C-NOT gate, are easily realizable. The basic idea of the dipole blockade two-qubit gate is as follows: The first example is shown in Fig. 5(b). We consider that two atoms are individually addressable by an optical field in the strong blockade regime ($B \gg \Omega$) and that the state $|1\rangle$ is coupled to the Rydberg state $|r\rangle$ with excitation Rabi frequency Ω. Then, a sequence of three pulses (2,3,4) implements a two-qubit controlled-phase gate operation (C-PG), and in conjunction with this C-PG operation, when two Hadamard rotation operations (labeled by 1 and 5, both $\pi/2$ pulses) are applied on the qubit state of the target atom before and after the C-PG operation, respectively, the C-NOT gate is constructed [30].

Besides the two Hadamard operations, the C-PG operates as follows: The second pulse (π-pulse) acts on the control atom $|1\rangle \rightarrow |r\rangle$, the second one ($2\pi$-pulse, 3) on the target atom, and the third one (π-pulse, 4) again on the control atom, where the excitation and de-excitation cycle of the target atom corresponds to a 2π rotation of an effective spin 1/2 and the wave function of the target atom undergoes a π phase rotation. Therefore, if the control atom is initially in $|0\rangle$, the target atom picks up π phase shift. However, if it is in $|1\rangle$, no phase shift is induced because in that case, the target atom never occupies the Rydberg state $|r\rangle$ due to the dipole blockade.

Alternatively, a sequence of seven pulses in Fig. 5(c) also implements the C-NOT gate. The conditional excitation (the first pulse) of the control atom to $|r\rangle$, depending on its initial state $|0\rangle$ or $|1\rangle$, either implements or prevents the swap operation. The swap operation is implemented by the next five pulses (2-6) of the qubit state of the target atom. The last pulse conditional resets the control atom back to its initial state [77]. The experimental demonstration of the seven-pulse C-NOT gate operation was carried out by Isenhower *et al.* with a pair of rubidium atoms separated by 10 μm in far off resonance traps (FORTs) [52]. The hyperfine energy levels of $|f = 1, m_f = 0\rangle$ and $|f = 2, m_f = 0\rangle$ in the ground $|5s_{1/2}\rangle$ are the two-level qubit bases. When the atoms were then excited to $n = 97$ Rydberg states by two photon excitation via $|5p_{3/2}\rangle$, the blockade shift was retained at $B/2\pi = 9.3$ MHz, which limited the double-excitation probability to $\Omega^2/(2B)^2 < 2.6 \times 10^{-3}$. In that case, the Rydberg excitation Rabi frequency was $\Omega/2\pi = 0.67$ MHz. During the C-NOT gate operation time of 7 μs, a fidelity of $F = 0.73$ was achieved. The experimental scheme is illustrated in Fig. 1.

More complex quantum gates can also be considered with Rydberg atoms. For example, the three-qubit Toffoli gate computes $t \rightarrow c_1 c_2 \oplus t$ for a given set of two control bits c_1 and c_2 and a target bit t. Thus, the target bit t is switched between 0 and 1 if both the control bits c_1 and c_2 are in state 1, and if either one of the control bits is in state 0, the target bit is unchanged. This gate has been designed with seven laser pulses, all of which are π pulses, in a three-Rydberg-atom system [78]. In this scheme, the three atoms are excited in different Rydberg energy levels, which enables the design of a more complex set of three-qubit gate operations.

While the previous example dealt with a system of multiple control bits and a single target bit, the opposite case, *i.e.,* a system of a single control bit and multiple target bits, also brings new applications of quantum information processing. In proposal termed as "mesoscopic Rydberg gates," a system in which a single atom (the control bit) is separated from and is singly addressable with respect to a mesoscopic ensemble of atoms (target bits) is considered [79]. The candidates for such a system include two-dipole-trap systems, large-spacing optical lattices, and magnetic trap arrays. We consider the system to be initially in the state $|c\rangle \otimes |t^N\rangle$, where the control bit $|c\rangle$ is the superposition state of $|0\rangle$ and $|1\rangle$, and $|t^N\rangle$ represents the mesoscopic state of the target ensemble of N atoms in state $|t\rangle$. Suppose now the C-NOT operation is applied with the sequence of laser interactions in Fig. 5(a) among the control and the target atoms, the Rydberg dipole blockade effect facilitates the C-NOT operation to all the target atoms simultaneously, which results in the output state becoming

$$(\alpha|0\rangle + \beta|1\rangle) \otimes |t^N\rangle \rightarrow \alpha|0\rangle \otimes |t^N\rangle + \beta|1\rangle \otimes |\bar{t}^N\rangle. \quad (13)$$

When $\alpha = \beta = 1/\sqrt{2}$ and $t = 0$ are given, for instance, the result in Eq. (13) is the well-known Greenberger-Horne-Zeilinger state [80], the maximally-entangled multi-partitite quantum state.

VIII. CONCLUSIONS

In conclusion, we have summarized the rapidly-growing research field of cold Rydberg atoms. The special properties of Rydberg atoms, *i.e.*, their extreme polarizability, long-range interaction, and long lifetime, have place them at the centers of highly-active research areas of modern atomic physics and quantum information science. During the last fifteen years, previously unknown types of novel matter, such as Rydberg molecules, cold neutral plasmas, and collective Rydberg matter, have been endlessly created one by one from vapors of cold Rydberg atom. Also, the atom-atom and atom-photon interactions in cold Rydberg atom systems have been successfully programmed to perform special functions in quantum-based technologies. The optical controllability of the Rydberg atom interaction may become ease and precise compared to the electric controllability

of electron devices. We hope that various entrancing applications of Rydberg-atom-based quantum technology will be realized in the future.

ACKNOWLEDGMENTS

This work was supported in part by Basic Science Research Programs [2010-0013899, 2009-0083512] and in part by World Class Insitute Program [WCI 2011-001] through the National Research Foundation of Korea.

REFERENCES

[1] T. F. Gallagher, *Rydberg Atoms* (New York: Cambridge University Press, 1994).
[2] J.-P. Connerade, *Highly Excited Atoms* (Cambridge University Press, Cambridge, 1998).
[3] R. F. Stebbings and F. B. Dunning, *Rydberg States of Atoms and Molecules* (Cambridge University Press, Cambridge, 1983).
[4] H. E. White, *Introduction to Atomic Spectra* (McGraw-Hill, New York, 1934).
[5] J. R. Rydberg, Phil. Mag. 5'th Ser, **43**, 390 (1883).
[6] M. L. Zimmerman, M. G. Littman, M. M. Kash and D. Kleppner, Phys. Rev. A **20**, 2251 (1979).
[7] T. Pohl, H. R. Sadeghpour and P. Schmelcher, Phys. Rep. **484**, 181 (2009).
[8] K. B. MacAdam, D. A. Crosby and R. Rolfes, Phys. Rev. Lett. **44**, 980 (1980).
[9] T. F. Gallagher, G. A. Ruff and K. A. Safinya, Phys. Rev. A **22**, 843 (1980).
[10] J. L. Dexter and T. F. Gallagher, Phys. Rev. A **35**, 1934 (1987).
[11] Y. N. Gnedin, A. A. Mihajlov, L. M. Ignjatović, N. M. Sakan, V. A. Sreković, M. Y. Zakharov, N. N. Bezuglov and A. N. Klycharev, New Astro. Rev. **53**, 259 (2009).
[12] A. Dalgarno, in *Rydberg States of Atoms and Molecules,* edited by R. F. Stebbings and F. B. Dunning (Cambridge University Press, Cambridge, 1983).
[13] J. A. Yeazell and C. R. Stroud, Jr., Phys. Rev. Lett. **60** 1494 (1988).
[14] R. R. Jones, Phys. Rev. Lett. **77**, 2420 (1996).
[15] J. Ahn, D. N. Hutchinson, C. Rangan and P. H. Bucksbaum, Phys. Rev. Lett. **86**, 1179 (2001).
[16] J. M. Raimond, M. Brune and S. Haroche, Rev. Mod. Phys, **73**, 565 (2001).
[17] S. Gleyzes, S. Kuhr, C. Guerlin, J. Bernu, S. Deléglise, U. B. Hoff, M. Brune, J.-M. Raimond and S. Haroche, Nature **446**, 297 (2007).
[18] H. J. Matcalf, *Laser Cooling and Trapping* (Springer-Verlag, New York, 1999).
[19] C. E. Wieman, D. E. Pritchard and D. J. Wineland, Rev. Mod. Phys. **71**, S253 (1999).
[20] W. R. Anderson, J. R. Veale and T. F. Gallagher, Phys. Rev. Lett. **80**, 249 (1998).
[21] I. Mourachko, D. Comparat, F. de Tomasi, A. Fioretti, P. Nosbaum, V. M. Akulin and P. Pillet, Phys. Rev. Lett. **80**, 253 (1998).
[22] M. P. Robinson, B. L. Tolra, M. W. Noel, T. F. Gallagher and P. Pillet, Phys. Rev. Lett. **85**, 4466 (2000).
[23] C. H. Greene, A. S. Dickinson and H. R. Sadeghpour, Phys. Rev. Lett. **85**, 2458 (2000).
[24] V. Bendkowsky, B. Butscher, J. Nipper, J. P. Shaffer, R. Löw and T. Pfau, Nature **458**, 1005 (2009).
[25] E. L. Hamilton, C. H. Greene and H. R. Sadeghpour, J. Phys. B: At. Mol. Opt. Phys. **35**, L199 (2002).
[26] C. Greene, A. S. Dickinson and H. R. Sadeghpour, Phys. Rev. Lett. **85**, 2458 (2000).
[27] S. T. Rittenhouse and H. R. Sadeghpour, Phys. Rev. Lett. **104**, 243002 (2010).
[28] M. D. Lukin, M. Fleischhauer, R. Cote, L. M. Duan, D. Jaksch, J. I. Cirac and P. Zoller, Phys. Rev. Lett. **87**, 037901 (2001).
[29] E. Urban, T. A. Johnson, T. Henage, L. Isenhower, D. D. Yavuz, T. G. Walker and M. Saffman, Nature **5**, 110 (2009).
[30] M. Saffman, T. G. Walker and K. Moelmer, Rev. Mod. Phys. **82**, 2313 (2010).
[31] H. Weimer, M. Müller, I. Lesanovsky, P. Zoller and H. P. Büchler Nat. Physics **6**, 382 (2010).
[32] K. D. Nelson, X. Li and D. S. Weiss, Nat. Physics **3**, 556 (2007).
[33] S. Whitlock, R. Gerritsma, T. Fernholz and R. J. C. Spreeuw, New J. Phys. **11**, 023021 (2009).
[34] P. Schaub, M. Cheneau, M. Endres, Ta.Fukuhara, S. Hild, A. Omran, T. Pohl, C. Gross, S. Kuhr, and I. Bloch, Nature **491**, 87 (2012).
[35] D. Comparat and P. Pillet, J. Opt. Soc. Amer. B **27**, A208 (2010).
[36] J. H. Choi, B. Knuffman, T. C. Leivisch, A. Reinhard and G. Raithel, Adv. At. Mol. Phys. **54**, 131 (2006).
[37] T. C. Killian, T. Pattard, T. Pohl and J. M. Rost, Phys. Rep. **449**, 77 (2007).
[38] D. B. Branden, T. Juhasz, T. Mahlokozera, C. Vesa, R. O. Wilson, M. Zheng, A. Kortyna and D. A. Tate, J. Phys. B **43**, 015002 (2010).
[39] Z. G. Feng, L. J. Zhang, J. M. Zhao, C. Y. Li and S. T. Jia J. Phys. B: At. Mol. Phys. **42**, 145303 (2009).
[40] V. S. Bagnato and L. G. Marcassa, Opt. Commun. **184**, 385 (2000).
[41] M. J. Seaton, Rep. Prog. Phys. **46**, 167 (1983).
[42] W. H. Li, I. Mourachko, M. W. Noel and T. F. Gallagher, Phys. Rev. A **67**, 52502 (2003).
[43] J. Zhao, H. Zhang, Z. Feng, X. Zhu, L. Zhang, C. Li and S. Jia, J. Phys. Soc. Japan **80**, 034303 (2011).
[44] K. Singer, M. Reetz-Lamour, T. Amthor, L. G. Marcassa and M. Weidemüller, Phys. Rev. Lett. **93**, 163001 (2004).
[45] D. Tong, S. M. Farooqi, J. Stanojevic, S. Krishnan, Y. Zhang, R. Côté, E. E. Eyler and P. L. Gould: Phys. Rev. Lett. **93**, 063001 (2004).
[46] M. G. Littman, M. M. Kash and D. Kleppner, Phys. Rev. Lett. **41**, 103 (1978).
[47] J. E. Bayfield and P. M. Koch, Phys. Rev. Lett. **33**, 258 (1974).
[48] J. C. Castro, M. L. Zimmerman, R. G. Hulet, D. Kleppner and R. R. Freeman, Phys. Rev. Lett. **45**, 1780 (1980).
[49] J. H. Choi, J. R. Guest, A. P. Povilus, E. Hansis and G. Raithel, Phys. Rev. Lett. **95**, 243001 (2005).
[50] J. R. Guest, J. H. Choi, E. Hansis, A. P. Povilus and G. Raithel, Phys. Rev. Lett. **94**, 073003 (2005).
[51] D. D. Yavuz, P. B. Kulatunga, E. Urban, T. A. Johnson,

N. Proite, T. Henage, T. G. Walker and M. Saffman Phys. Rev. Lett. **96**, 063001 (2006).
[52] L. Isenhower, E. Urban, X. L. Zhang, A. T. Gill, T. Henage, T. A. Johnson, T. G. Walker, M. Saffman, Phys. Rev. Lett. **104**, 010503 (2010).
[53] Gaëtan, A., Y. Miroshnychenko, T. Wilk, A. Chotia, M. Viteau, D. Comparat, P. Pillet, A. Browaeys and P. Grangier, Nat. Physics **5**, 115 (2009).
[54] S. M. Farooqi, D. Tong, S. Krishnan, J. Stanojevic, Y. P. Zhang, J. R. Ensher, A. S. Estrin, C. Boisseau, R. Côté, E. E. Eyler and P. L. Gould, Phys. Rev. Lett. **91**, 183002 (2003).
[55] K. R. Overstreet, A. Schwettmann, J. Tallant and J. P. Shaffer, Phys. Rev. A **76**, 011403 (2007).
[56] T. C. Killian, S. Kulin, S. D. Bergeson, L. A. Orozco, C. Orzel and S. L. Rolston Phys. Rev. Lett. **83**, 4776 (1999).
[57] L. A. Girifalco, *Statistical mechanics of solids.* (Oxford University Press, Oxford, 2003).
[58] T. Pohl, T. Pattard and J. M. Rost, Phys. Rev. A **70**, 033416 (2004).
[59] S. Kulin, T. C. Killian, S. D. Bergeson and S. L. Rolston, Phys. Rev. Lett. **85**, 318 (2000).
[60] X. L. Zhang, R. S. Fletcher and S. L. Rolston, Phys. Rev. Lett. **101**, 195002 (2008).
[61] M. Walhout, H. J. L. Megens, A. Witte and S. L. Rolston, Phys. Rev. A **48**, 879 (1993).
[62] T. C. Killian, Y. C. Chen, P. Gupta, S. Laha, Y. N. Martinez, P. G. Mickelson, S. B. Nagel, A. D. Saenz and C. E. Simien, J. Phys. B: At. Mol. Opt. Phys. **38**, 351 (2005).
[63] E. A. Cummings, J. E. Daily, D. S. Durfee and S. D. Bergeson, Phys. Rev. Lett. **95**, 235001 (2005).
[64] A. Walz-Flannigan, J. R. Guest, J.-H. Choi and G. Raithel, Phys. Rev. A **69**, 63405 (2004).
[65] D. Ciampini, M. Anderlini, J. H. Muller, F. Fuso, O. Morsch, J. W. Thomsen and E. Arimondo, Phys. Rev. A **66**, 043409 (2002).
[66] S. D. Bergeson and R. L Spencer, Phys. Rev. E **67**, 026414 (2003).
[67] R. S. Fletcher, X. L. Zhang and S. L. Rolston, Phys. Rev. Lett. **96**, 105003 (2006).
[68] J. Castro, P. McQuillen and T. C.. Killian, Phys. Rev. Lett. **105**, 065004 (2006).
[69] P. McQuillen, J. Castro and T. C. Killian, J. Phys. B: At. Mol. Opt. Phys. **44**, 184013 (2010).
[70] D. Jaksch, J. I. Cirac, P. Zoller, S. L. Rolston, R. Côté and M. D. Lukin, Phys. Rev. Lett. **85**, 2208 (2000).
[71] M. A. Nielsen and I. L. Chuang, *Quantum Computation and Quantum Information* (Cambridge University Press, Cambridge, England, 2000).
[72] M. L. Citron, H. R. Gray, C. W. Gabel and C. R. Stroud, Jr., Phys. Rev. A **16**, 1507 (1977).
[73] T. Vogt, M. Viteau, J. Zhao, A. Chotia, D. Comparat and P. Pillet, Phys. Rev. Lett. **97**, 083003 (2006).
[74] M. Reetz-Lamour, T. Amthor, J. Deiglmayr and M. Weidemüller, Phys. Rev. Lett. **100**, 253001 (2008).
[75] R. Löw, H. Weimer, U. Krohn, R. Heidemann, V. Bendkowsky, B. Butscher, H. P. Büuchler and T. Pfau, Phys. Rev. A **80**, 033422 (2009).
[76] M. P. A. Jones, J. Beugnon, A. Gaëtan, J. Zhang, G. Messin, A. Browaeys and P. Grangier, Phys. Rev. A **75**, 040301 (2007).
[77] N. Ohlsson, R. K. Mohan and S. Kröll, Opt. Commun. **201**, 71 (2002),
[78] E. Brion, A. S. Mouritzen and K. Mölmer, Phys. Rev. A **76**, 022334 (2007).
[79] M. Müller, I. Lesanovsky, H. Weimer, H. P. Büuchler and P. Zoller, Phys. Rev. Lett. **102**, 170502 (2009).
[80] D. Greenberger, M. Horne, A. Shimony and A. Zeilinger, Am. J. Phys. **58**, 1131 (1990).